

CORPHAD and METCOR ISTC projects

S.V. Bechta¹, V. B. Khabensky¹, V.S. Granovsky¹, E.V. Kroushinov¹, S.A. Vitol¹,
V.V. Gusarov², V.I. Almiyashev², L.P. Mezentseva², Yu. B. Petrov¹⁰, D.B. Lopukh¹⁰,
M. Fischer³, D. Bottomley⁴, W. Tromm⁵, M. Barrachin⁷,
E. Altstadt⁹, P. Piluso⁶, F. Fichot⁷, S. Hellmann³, F Defoort⁸

- | | |
|--------------------------------|---------------------------------|
| 1) NITI, Sosnovy Bor (RU) | 6) CEA/DEN, Cadarache (FR) |
| 2) ISC RAS, St Petersburg (RU) | 7) IRSN, Cadarache (FR) |
| 3) FRAMATOME ANP Erlangen (DE) | 8) CEA/DEN, Grenoble (FR) |
| 4) ITU, Karlsruhe (DE) | 9) FZR, Dresden (DE) |
| 5) FZK, Karlsruhe (DE) | 10) SPGETU, St. Petersburg (RU) |

SUMMARY

The ongoing CORPHAD Project (Phase Diagrams for Multicomponent Systems Containing Corium and Products of its Interaction with NPP Materials) started in August 2001. The main aim of the project is to experimentally determine the relevant physicochemical data on phase diagrams of binary, ternary, quaternary and prototypic multi-component systems, which are important for analysis and modelling of a severe accident (SA) and efficient planning of severe accident management (SAM) measures. The data should be directly used for the European NUCLEA database development and validation. The following systems are in the focus of the project: (1) $UO_2 - FeO$, (2) $ZrO_2 - FeO$, (3) $SiO_2 - Fe_2O_3$, (4) $UO_2 - SiO_2$, (5) $UO_2 - ZrO_2 - FeO$, (6) $UO_2 - ZrO_2 - FeO_y$, (7) U-O-Fe, (8) Zr-O-Fe, (9) U-O-Zr, (10) U-Zr-Fe-O, (11) complex corium mixtures.

The experimentally determined data of the listed diagrams include: coordinates of characteristic points (eutectics, peritectics and others); liquidus and solidus concentration curves; component solubility limits in the solid phase; tie line coordinates and temperature-concentration regions of the miscibility gap. Different methodologies are used for the phase diagram study. Classical methods of thermal analysis, like DTA and DSC are combined with methods specifically developed for corium studies.

The METCOR project (Investigation of Corium Melt Interaction with NPP Reactor Vessel Steel) started in April 1999. The objectives of the project are to qualify and to quantify physico-chemical phenomena of corium melt interaction with reactor vessel steel cooled from the outside. The variable parameters of the interaction tests are: oxygen potential in the system, corium composition, interaction interface temperature and heat flux from corium to steel. The medium scale tests with corium mass of about 2 kg are carried out by using high-frequency induction heating of the corium melt in a cold crucible.

The METCOR & CORPHAD work-packages are performed by Russian partners in close collaboration with leading European scientific institutes in the area of corium research as well as with the European nuclear industry.

This paper briefly describes the results obtained in both projects and their possible application for SA analysis and SAM. The paper concludes with recommendations for future research activities in the framework of METCOR and CORPHAD projects.

A. INTRODUCTION

The integrated approach, which is currently in use for SA analysis and SAM is generally based on the coupling of thermal hydraulics and physical chemistry (Ref. [1]). This requires a better knowledge of physicochemical phenomena playing an important role in an accident scenario and in determining in/ex-vessel corium behaviour. The starting point for physicochemical modeling are phase diagrams of corium and its mixture with structural materials. For in-vessel conditions such a mixture generally corresponds to U-Zr-Fe (Cr, Ni, Mn...)-O system. For ex-vessel corium the chemical system is even more complicated and additionally contains different elements of surrounding structures, e.g. Si, Al, Ca, Mg and others from reactor pit concrete or sacrificial material of a core catcher (Ref.[2], [3]).

The intensive development of theoretical methods of phase diagram calculation and their application in modeling of severe accident phenomena are currently underway. These efforts have resulted in various numerical codes (Ref. [4]), such as GEMINI (Ref. [5]), MULTICOM (Ref. [6]) and code-oriented databases like IVTANTHERMO (Ref. [7]) and NUCLEA (Ref. [8]). The validation of phase diagram databases requires experimental support focused on studying the still unexamined high-temperature systems or domains and refining the available data. Owing to the EU support, in recent years the work on NPP safety, and phase diagram investigations in particular, has been integrated in large international projects like CIT (Corium Interaction and Thermochemistry), THMO (Thermochemical Modeling and Data), ENTHALPY (Constitution of a European Nuclear Thermodynamic Database Validated and Applicable in Severe Accidents, NUCLEA), SARNET (Severe Accident Research NETWORK of excellence) and several ISTC (International Science and Technology Center) projects. The ISTC CORPHAD project is focused on the European NUCLEA database improvement and validation.

Knowledge of the phase diagrams enables modeling of equilibrium conditions. For corium/material interaction and for in-vessel retention (IVR) in particular these conditions can be reached after several hours. Modeling of transients is based on the kinetic data of corium/material interaction, e.g. interaction of corium melt with reactor vessel steel cooled from outside. The ISTC METCOR project deals with experimental studies of such interactions.

B. CORPHAD PROJECT

The objective of the CORPHAD project is the experimental determination of phase diagram data important for reactor application, phase diagram modeling and NUCLEA database optimization.

The list of phase diagrams and current status of separate diagram research are presented in the test matrix (Table 1). According to the matrix, the step by step study of more and more complicated system starts from quasi binary oxide systems, continues to ternary oxide, or metal/oxide systems with miscibility gap and then a quadruple system, which is basic system considered for IVR, and concludes by a complex prototypic ex-vessel corium.

Table 1: CORPHAD test matrix

Task	System	Atmosphere	Status
1	UO ₂ – FeO	Argon	Completed
	ZrO ₂ – FeO		
	SiO ₂ – Fe ₂ O ₃	Air/ oxygen	
	UO ₂ – SiO ₂	Argon /Air	In preparation
2	UO ₂ – ZrO ₂ -FeO (only eutectic point measurements)	Argon	Completed
	UO ₂ – ZrO ₂ -FeO _y (only eutectic point measurements)	Air	
	U-O-Fe	Argon	In progress
	Zr-O-Fe		
	U-O-Zr		
3	U-Zr-Fe-O		In preparation
4	Complex corium mixture (only eutectic point measurements)	Air	

B.1 Methodology

The specimens were prepared from oxide powders and metal charges of high purity. Controlled gas atmospheres (Ar/H₂, Ar, air and oxygen) and small quantities of metal getter (Fe) were used for maintenance of the specific system stoichiometry. The chemical composition of the specimens was determined by X-ray fluorescence (XRF), spectrophotometry and gas-volumetry using methodologies described in Ref. [9-11]. The phases of the specimens were identified by X-ray diffraction (XRD). The microstructure, elemental composition of the specimens and the composition of different phases were determined by scanning electron microscopy (SEM) and energy-dispersion micro analysis (EDX) using two scanning electron microscopes; either the CamScan MV2300 or the AVT-55 equipped with Oxford Link micro-analysis devices.

It should be stressed that the surface and chemical activity of melts in the studied systems restrict the possibilities of using classical methods of thermal analysis because of the melt interaction with crucible materials (Al₂O₃, ZrO₂, W, W/Re, Ir, etc.). DTA/DSC and other crucible-based methods can be used only in very limited composition and temperature ranges (in most cases for solidus temperature determination only). That is why we also used specially adapted methods, which have been originally elaborated and developed at NITI (Academician Alexandrov Research Institute of Technology) and ISC RAS (Institute of Silicate Chemistry of Russian Academy of Sciences). Just an overview of methods used and certain details of their application will be given here. The original experimental facilities and methodologies are described in details in [Ref. 12].

Specimens were produced by the method of induction melting in a cold crucible (IMCC) at the RASPLAV-2 and RASPLAV-3 test facilities. Determination of solidus (T_{sol}) and liquidus (T_{liq}) temperatures for the majority of compositions was carried out by the method of visual polythermal analysis (VPA) also using RASPLAV facilities (VPA IMCC,

Fig. 1(a), Ref.[13]) and VPA in the Galakhov microfurnace (Fig. 1(b), Ref. [14]).

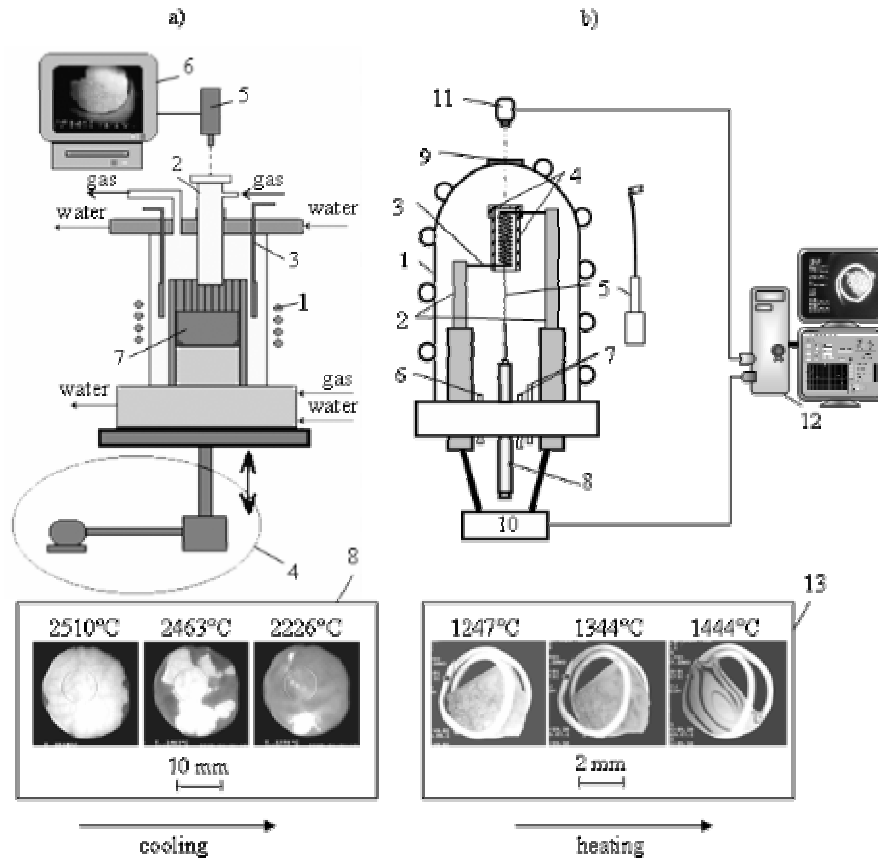


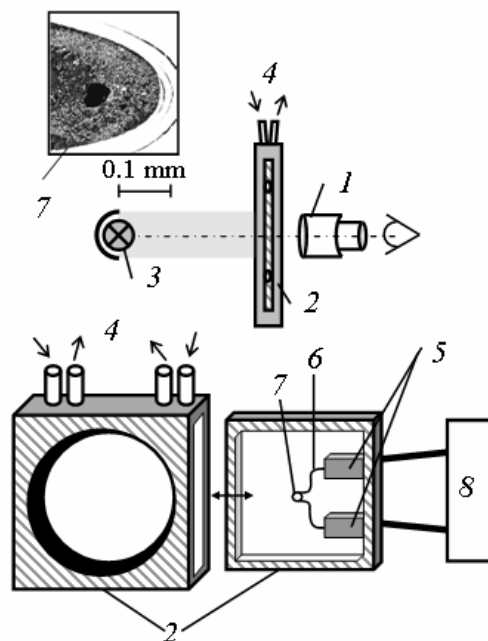
Fig. 1 (a, b): Schematics of Visual Polythermal Analysis facilities: a) – Induction Melt in Cold Crucible facility “Rasplav 3”: 1- inductor, 2 – pyrometer shaft, 3 – movable water-cooled electromagnetic screen, 4 – crucible vertical shift drive, 5 – pyrometer coupled with a videocamera, 6 – control and registration system, 7 – melt, 8 – cooled molten pool surface in the sighting spot; **b) – Galakhov microfurnace:** 1 – water-cooled sealed body, 2 – steel electrodes, 3 – tungsten heating coil, 4 – molybdenum protective screens, 5 – specimen holder (iridium or molybdenum), 6 – pumping-out system, 7 – gas flooding system, 8 – specimen quenching device, 9 – quartz viewing port, 10 – regulated power sources, 11 – videocamera, 12 – observation and control system, 13 – view of a specimen in the holder during heating.

For the T_{liq} determination by VPA IMCC, the molten pool surface temperature was measured by the spectral ratio pyrometer at the instant of the solid phase appearance in the pyrometer sighting spot (Fig. 1a, 8 – middle frame). The appearance of the solid phase nuclei on the locally cooled surface of the volumetrically superheated molten pool was recorded with a high speed digital video camera and the images were subjected to a frame-by-frame analysis. The maximum error of T_{liq} measurement by this method for the compositions with a big $T_{sol}-T_{liq}$ difference is not more than 50-75°C, but usually the error is significantly smaller. It should be noted that regardless of the compositions and temperatures, the VPA IMCC application ensures the absence of interaction between the crucible materials and the melt and of contamination of the melt by corrosion products.

For VPA in the Galakhov microfurnace, fragments of the ingot prepared by IMCC, weighing 7 to 8 mg each, were taken and fixed between the coils of the holder located in the isothermal microfurnace zone (Fig. 1b). The effective range of temperature measurements in

the microfurnace is between 900-2500°C with an error of around $\pm 30^\circ\text{C}$ [Ref. 14]. The measurements were made in a neutral atmosphere (high-purity helium under $0.25 \cdot 10^5$ Pa (0.25 bar) for the low-temperature domains, an argon-hydrogen mixture, 96 vol. % Ar – 4 vol. % H_2 , under $1.25 \cdot 10^5$ Pa (1.25 bar) for the high-temperature domains). To avoid active interaction between the specimen and the holder, the latter was produced from iridium wire. Moreover the possible effect of the heating rate on the error of visual determination of the melting initiation temperature and the complete melting was checked and the optimal rate of 5°C/s was chosen near the critical points. The process of specimen melting was recorded with a digital video camera and the images subjected to a frame-by-frame analysis. T_{sol} was defined as the temperature at which sharp edges of the specimen started degrading during heating. T_{liq} was defined as the temperature of the specimen's complete melting and spreading across the holder (Fig. 1b, 13 – last frame). The microfurnace design allows quenching of specimens by dropping them together with the holder into the cold zone of the furnace. After quenching, the microstructure and elemental composition of the specimen's phases were analyzed.

VPA in conditions of high oxygen potential (e.g. in air, $p_{\text{O}_2} \approx 0.21 \cdot 10^5$ Pa, or in oxygen, $p_{\text{O}_2} \approx 1.0 \cdot 10^5$ Pa for $\text{SiO}_2\text{-Fe}_2\text{O}_3$ system study) was made also by using high temperature (HT) microscope (Fig. 1(c)). Powder samples of less than 1.0 mg were taken. The error of both T_{sol} and T_{liq} determination by this technique usually falls within the range $\pm 25\text{-}30^\circ\text{C}$ but may be more significant for highly viscous SiO_2 -containing melts. Besides, the measured temperature may be overestimated due to the high heating rate available on HT microscope. To avoid this, heating was made in stages, increasing at $5^\circ\text{C}\cdot\text{s}^{-1}$ for 500°C with about 10 s hold time in between every 500°C ramp. T_{sol} was determined at the very beginning of the visible shifting of the specimen mass towards the loop top or one of its sides as a consequence of the first liquid formation. The liquidus temperature was defined either as the temperature of melt drop spreading across the loop-like holder (7 in Fig. 1(b)), or, in cases of high silica content (i.e. high melt viscosity), as the temperature at which the melt became transparent.



1 – long-focus microscope, 2 – sealed heating chamber with quartz windows and sample holder cartridge, 3 – lighting system, 4 – gas tubes, 5 – silver electrodes, 6 – iridium loop heater (specimen holder), 7 – specimen (powder), 8 – power supply;

Fig. 1(b): Schematics of high-temperature microscope

As already mentioned, the solidus thermal effects and a limited number of liquidus effects at relatively low temperatures were studied by differential thermal analysis (DTA) using the SETARAM TAG-24 and NETZSCH STA 429 thermal analyzers. The temperatures of thermal effects were indicated by peaks in DTA curves and were determined by the tangential intercept of the 'thermal effect' curve and the baseline. The DTA tests were carried out with specimens weighing about 30 mg, typically heated at a rate of 10°C/min. All the specimens for DTA were prepared by quenching of the melt produced by the IMCC.

For the eutectic composition determination, slow melt crystallizations were performed in the IMCC, which ensured the displacement of a eutectic liquid by the crystallization front. As the more refractory materials crystallized out, the composition of the remaining liquid became closer and closer to that of the eutectic. The eutectic crystallization zone was recognized by its characteristic microstructure in the ingot. In order to determine the final solubility of components in the solid solutions additional experiments were performed in which the solid solution was kept in long-term contact with a melt having a near-eutectic composition.

The IMCC method enables the study of metal/oxide systems with miscibility gap, in particular U-O-Fe, Zr-O-Fe and U-O-Zr. Such melts can not be prepared neither in refractory metal nor in ceramic crucibles. In the performed tests the density difference between the two coexisting liquids was big enough and the molten pools in the cold crucible stratified with the less dense liquid on the top. The compositions of the top liquids were measured by melt sampling, quenching and post test analysis of the sample. Thus, the tie lines in the miscibility gap were determined. The critical points for these measurements are high precision of oxygen measurements in the metal and preparation of molten pool with a uniform temperature.

B.2 Results

The most important data obtained in CORPHAD for the systems, which have been studied (Table 1), are listed below.

UO₂ – FeO

For UO₂–FeO system phase diagram, the experimental data were scarce up to now. Some data have been obtained in the CIT project [22] in the FeO rich part of the system. In particular the eutectic composition and temperature have been approximately determined at 3.3% mole UO₂ and 1340°C. In CORPHAD, the phase diagram of the UO₂–FeO system has been constructed in details (Fig.2, Ref. [15]). The experimental investigation has confirmed that it is a diagram with an eutectic point. The eutectic temperature and composition of the system have been specified to be 1335±5°C and 3.9±0.5 mole %UO₂. This is in agreement with the previous data. A region of limited solid solutions of FeO in UO₂ has been shown. The final solubility of FeO in UO₂ at the eutectic temperature is evaluated as 17.0±1.0 mole %. The solidus and liquidus temperatures and specimen compositions determined by different methods are in good agreement to within the measurement errors. This consistency demonstrates the reliability of the presented values.

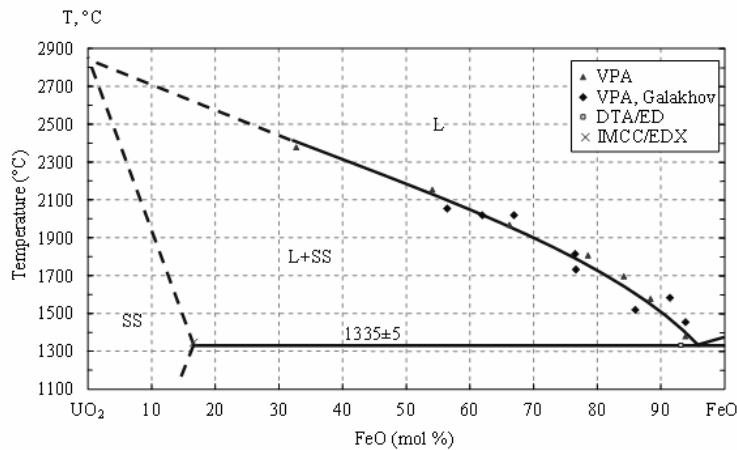


Fig. 2: Phase diagram of the UO₂-FeO system

ZrO₂ – FeO

For this phase diagram the experimental data were also scarce and uncertain. Fischer performed liquidus determination [23] yielding a eutectic point at 5% mole ZrO₂ and 1330°C and showing the existence of a domain of ZrO₂-based solid solution within 4% wt. FeO at 1450°C. More recently measurements were performed by Hellmann [24] in the CIT Project leading to lower liquidus temperatures than Fischer data. In CORPHAD the pseudobinary phase diagram of the ZrO₂-FeO system in inert atmosphere (Ar) has been precisely constructed (Fig. 3, Ref. [12]). The diagram has an eutectic point and a phase region of solid solution of FeO in ZrO₂. The eutectic composition and the eutectic temperature in the system have been specified. They correspond to (10.3±0.6) mol % ZrO₂ and (1332±5)°C. The parameters of the solid solution of FeO in ZrO₂ have been determined as follows:

- *t*-ZrO₂(FeO) exists in the temperature range from 1172 to 2347°C, the ultimate FeO solubility in *t*-ZrO₂ is (2.2±0.3) mol % at 1332°C;
- *c*-ZrO₂(FeO) exists in the temperature range from 1800 to 2710°C, the solubility limit of FeO in ZrO₂ at 1800°C is about 13 mol % FeO.

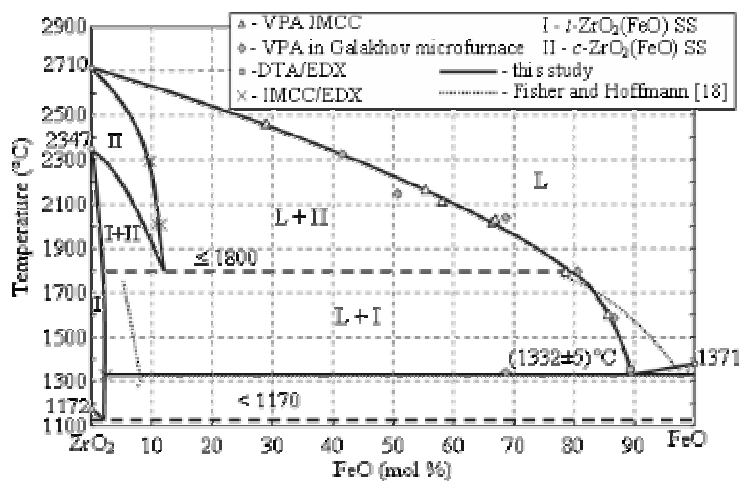


Fig. 3: Phase diagram of the ZrO₂-FeO system

SiO₂-Fe₂O₃(Fe₃O₄)

Very few data were available for the modelling of these systems. In the different published assessments, the SiO₂-Fe₂O₃ phase diagram is always represented with a miscibility gap in the liquid state but the characteristic points were not determined and strongly differed from one author to another one. The combination of the VPA (Galakhov microfurnace), DTA and SEM/EDX data allowed the phase diagram of the quasi-binary Fe₃O₄-SiO₂ system at $p_{O_2} \approx 1.0 \cdot 10^{-1}$ Pa to be constructed (Fig. 4, Ref. [16]). This is a diagram with one eutectic point at 1424 °C and 75±1 mol % FeO_{1.33}. The miscibility gap is found to occur within the concentration range approximately from 64 to 27 mol % FeO_{1.33} at the monotectic temperature 1550 °C. In the diagram the temperature of 1424 °C according to DTA/TG results is related to Fe₃O₄ dissociation accompanied with oxygen loss (1.1 %), FeO and first portions of liquid formation according to the Darken & Gurry's diagram (Ref. [17]). The X-ray pattern of the sample containing 96.2 mol % FeO_{1.33} indicates not only reflections of Fe₃O₄ but also of FeO and Fe₂SiO₄ formed during FeO and SiO₂ interaction. This confirms Fe₃O₄ dissociation process with FeO formation. At the same time this temperature (1424°C) is related to the solidus of the quasi-binary Fe₃O₄-SiO₂ system.

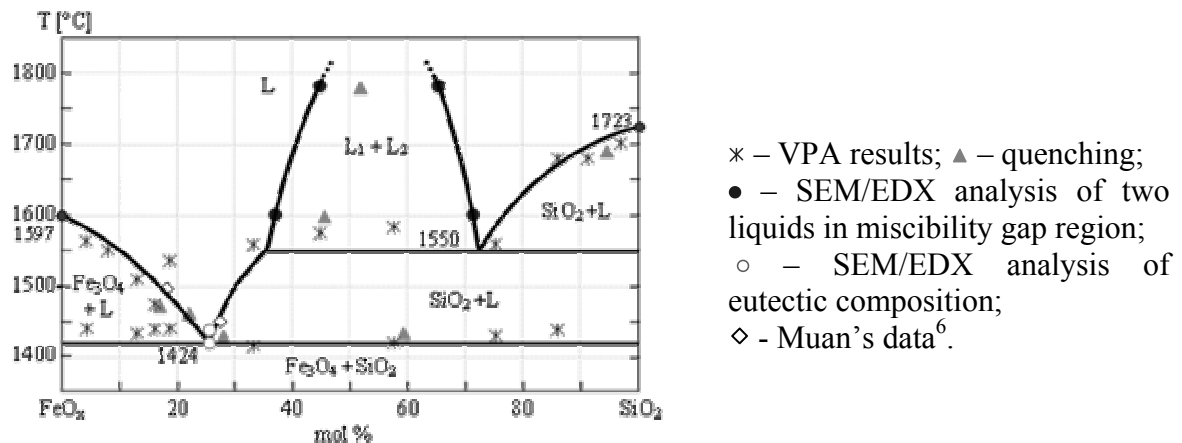


Fig. 4 : Phase diagram of the quasi-binary SiO₂-Fe₃O₄ system in neutral atmosphere (Galakhov microfurnace; $p_{O_2} \approx 1.0 \cdot 10^{-1}$ Pa)

The combination of the VPA (HT microscope) and DTA results allowed construction of the phase diagrams of the quasi-binary SiO₂-Fe₂O₃ system at $p_{O_2} \approx 0.21 \cdot 10^5$ Pa (Fig. 5(a), Ref. [16]) and $p_{O_2} \approx 1.0 \cdot 10^5$ Pa (Fig. 5(b), Ref. [16]). These are the diagrams with the same eutectic point corresponding to 1473±3 °C and 84.4±1 mol % FeO_{1.5}. The eutectic temperature determined by VPA (1470±25°C) was defined on the basis of the DTA results. The miscibility gap determined according to the liquidus line kink and the monotectic position was found in both diagrams to be within the concentration range from approximately 82.3 to 14.8 mol % FeO_{1.5} at 1535 °C. It should be pointed out that the T_{sol} and T_{liq} values obtained by the HT microscope in air and in oxygen were identical (Fig. 5).

The oxygen partial pressure affects the temperature of Fe₂O₃ decomposition at 1388°C into Fe₃O_{4+x}, which is characterized by reversible oxygen loss (Ref. [18]). Besides, the Fe₃O₄ phase should be nonstoichiometric (Fe₃O_{4+x}) under the experiment's conditions as is shown in Darken & Garry's diagram (Ref. [18]).

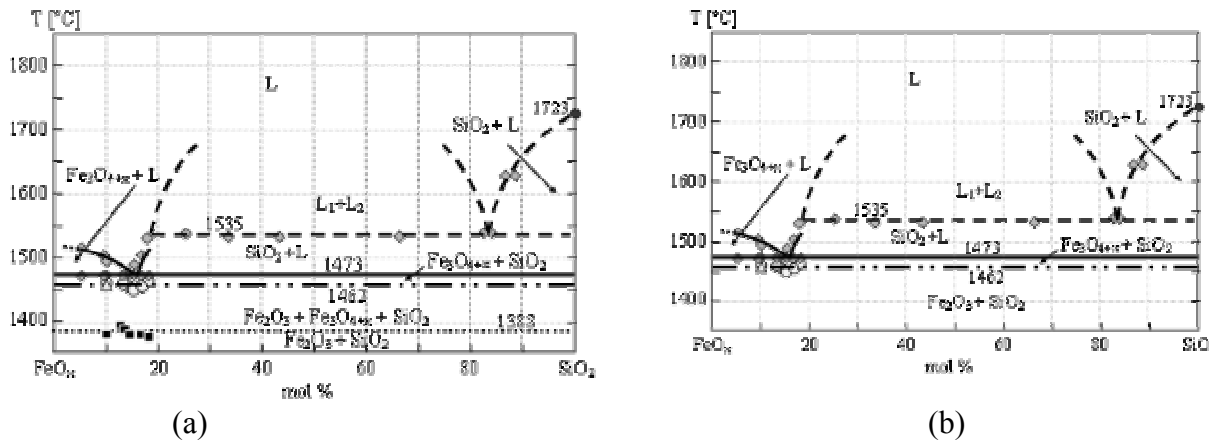


Fig. 5: Phase diagram of the quasibinary $\text{SiO}_2\text{-Fe}_2\text{O}_3$ system in air (a) and in oxygen (b); \diamond – HT microscope; \circ – DTA results on eutectic temperature; \blacksquare – DTA results on Fe_2O_3 decomposition temperature

C. METCOR PROJECT

The objectives of the tests (see Table 2) were to identify the interaction phenomena and to determine the kinetics and final corrosion depth. The interaction of oxidic corium $\text{UO}_2/\text{ZrO}_2/\text{FeO}(\text{Fe}_3\text{O}_4)$ with reactor steel in air and neutral (nitrogen) above-melt atmosphere was the subject of experimental investigations during the 1st phase of METCOR ISTC project. Its results have been published in Ref. [18], [19], and corrosion models developed on the basis of their results are given in Ref. [20]. The first results on the interaction of suboxidized and oxidized (C 30 and C 100) corium with vessel steel in neutral (argon) atmosphere carried out within the 2nd phase of METCOR ISTC project are given in Ref. [21].

Table 2: METCOR test matrix

Melt	Atmosphere	Status
$\text{UO}_2\text{-ZrO}_2\text{-FeO}_y$	nitrogen	Completed
$\text{UO}_{2+x}\text{-ZrO}_2\text{-FeO}_y$	air	
$\text{UO}_{2+x}\text{-ZrO}_2, \text{UO}_{2+x}\text{-ZrO}_2\text{-FeO}_y$	steam	In progress
$\text{UO}_2\text{-ZrO}_2, \text{UO}_2\text{-ZrO}_2\text{-Zr}$	argon	Completed
$\text{UO}_2\text{-ZrO}_2\text{-Zr-SS}$		

C.1 Methodology

The studies were performed at the “Raspilav-3” test facility, which uses the technique of IMCC for producing the corium melt. A schematic diagram is presented in Fig. 6. The furnace air-tightness was ensured by quartz tube (4) and water-cooled cover (2). Argon was supplied through a shaft (1) with its own gas flow in order to remove aerosols and thus improve the quality of pyrometry and video recording. Steel specimens were fabricated from parts of a VVER-1000 reactor vessel made from 15Kh2NMFA steel, with embedded K-type thermocouples at different distances from the top and from the axis. An acoustic defect was made near the specimen top, it was a circular (\varnothing 2mm) borehole. The defect was used for ultrasonic measurements of specimen ablation kinetics. Top (12) and bottom (13) calorimeters (Fig. 6) were provided for cooling the specimen, in particular the zone where it was connected to the ultrasonic sensor. The calorimeters were also used for measuring melt – specimen heat fluxes. The following in-situ measurements were carried out during the tests:

- coolant temperature and flow rates;

- melt surface temperatures;
- temperature distribution in the steel specimen;
- steel specimen corrosion depth;
- electrical characteristics of the IMCC power supply.

Main parameters to be varied during the tests (Table 2) were: corium composition and melt oxygen potential (or oxidation index C), temperature of corium/steel interaction interface and heat flux density from corium to steel. Posttest analysis included numeric modeling of the specimen temperature field. To study the vessel steel-corium interaction zone the prepared corium-steel templates and the corium samples taken during the test were subjected to posttest physicochemical analyses to determine their elemental and phase compositions, microstructure and material properties.

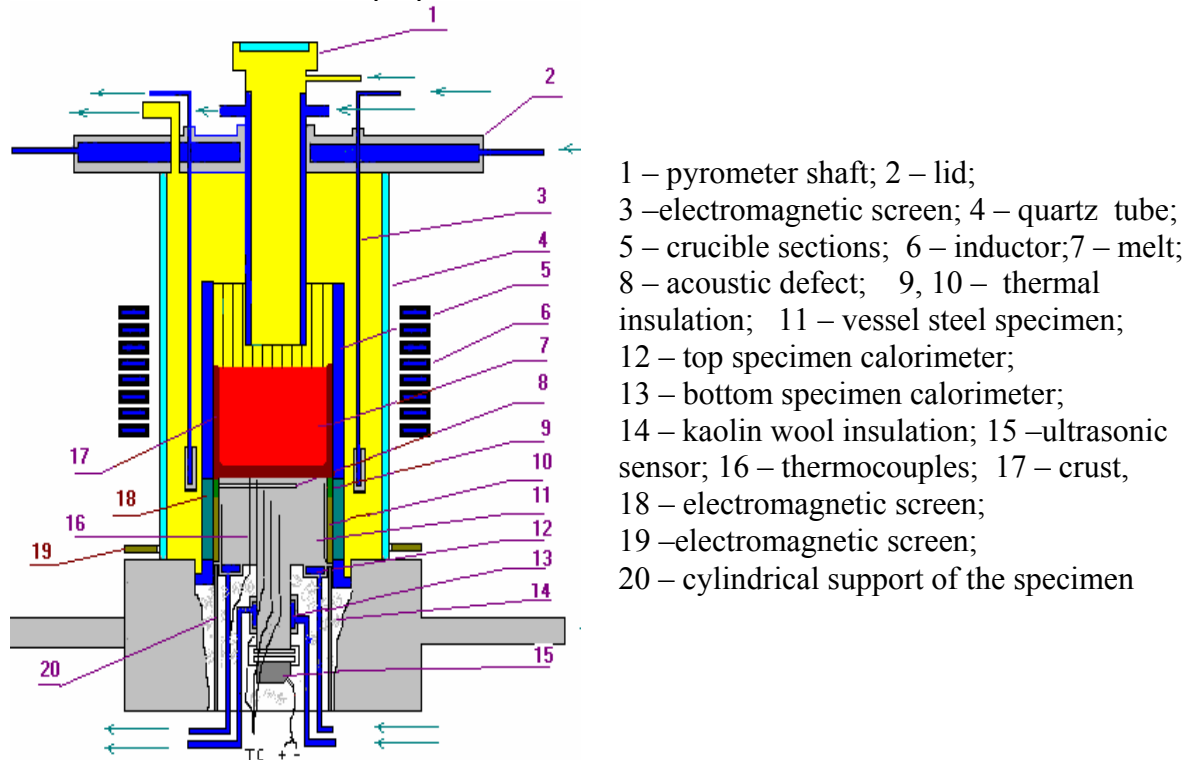


Fig. 6: Furnace schematics.

The following methods were used:

- 1) Analysis of elementary composition: X-ray fluorescence (XRF), Chemical analysis – spectrophotometry.
- 2) Analysis of phase composition: EDX analysis.
- 3) Metallo- and ceramography: Optical microscopy, Scanning electron microscopy (SEM).

Corium oxidation degree and content of free zirconium in samples were determined by:

- A gas-volumetric method for the determination of Zr content from the volume of hydrogen release during the reaction with phosphoric acid,
- Photocolorimetry of uranium (IV) and uranium (VI) with arsenazo III reagent.

C.2 Results

Two basically different mechanisms of vessel steel ablation at a high and low oxygen potential of the melt have been identified. At high oxygen potential ($C > 100$) the ablation is caused by high temperature surface oxidation (corrosion) of steel and the limiting diffusion

barrier is the iron oxide surface layer. In conditions of low melt oxygen potential ($C < 100$), the interaction of corium with steel components intensifies as a result of eutectic mechanism with formation of a metallic U-Zr-Fe-(O) mushy zone, which dilutes the steel cooled from outside upto the isotherm of solidus temperature of the mushy zone composition. For all the tests this temperature was in the range 1090-1200 C, which is significantly lower than the steel melting point.

The obtained results enable us to qualitatively estimate the influence of the melt oxidation index C (Ref. [21]) on the steel ablation rate. This is depicted in Fig. 7 and shows the minimum rate at the point of corium full stoichiometry and increasing corrosion rate with deviation from this point.

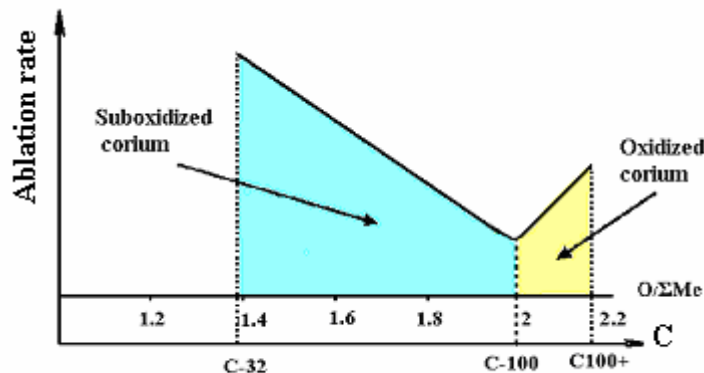


Fig. 7 Influence of the corium melt oxidation index C on steel ablation rate

Considering the possible application of METCOR results for SA analysis and SAM it should be emphasized that, for low and medium capacity reactors, IVR at low circuit pressure will not be critically impacted by the identified new phenomena, as the high strength of material of the outside “cold” steel layer of the vessel wall is not affected. However, if the pressure in the vessel will be high enough, the oxidized/dissolved layer of the steel can be critical for the vessel’s mechanical behaviour and the position of maximum material damage. In this context it should be noted, that oxidation/corrosion phenomena in its turn can be sensitive to strains in the vessel steel.

D. CONCLUSIONS

Considerable progress has been made in CORPHAD and METCOR projects. CORPHAD data for binary oxide systems have been already used for NUCLEA optimization. There is still lack of knowledge for several systems, which are of high importance for reactor application and NUCLEA improvement, it is therefore reasonable to extend the application of the developed methodology and to study in more detail: U-Zr-O, U-Fe-O, Zr-Fe-O, U-Zr-Fe-O, UO_2-SiO_2 , CaO - UO_2 , CaO - FeO, $UO_2 - FeO - SiO_2$, $UO_2 - FeO - CaO$, $ZrO_2 - FeO - SiO_2$ and $ZrO_2 - FeO - CaO$ systems.

METCOR project perspectives are related to study of some remaining, but important IVR uncertainties, particularly of corium/vessel steel interaction at the vertical orientation of the interface, at melt oxidation transients and to application of the testing the vessel steel of European PWR reactors.

REFERENCES

- [1] J.M. Seiler, K. Froment “Material Effects on Multiphase Phenomena in Late Phase of Severe Accidents of Nuclear Reactors”, *Multiphase Science and Technology*, Vol. 12, no. 2, pp. 117-257, 2000
- [2] A.A. Sulatsky, S.V. Behta, V.S. Granovsky, V.B. Khabensky, E.V. Krushinov, S.A. Vitol, V.V. Gusarov, V.I. Almjashev, P.V. Bezlepkin “Molten Corium Interaction with Oxidic Sacrificial Material of VVER Core Catcher”, *Proceedings of ICAPP '05*, Paper 5240, Seoul, KOREA, May 15-19, 2005
- [3] M. Fischer “The Severe Accident Mitigation Concept and the Design Measures for Core Melt Retention of the EPR”, *NED*, 230 (2004), pp. 169-180
- [4] G.V. Belov, *Thermodynamic modeling: methods, algorithms, software*, Nauchny Mir Publishers, Moscow, 2002 (Rus.)
- [5] B. Cheynet, P.Y. Chevalier, E. Fischer, *Thermosuite*, *CALPHAD* 26 (2002) 167-174
- [6] O.V. Mazurin, V.V. Gusarov, *The future of information technologies in material studies*, *Glass physics and chemistry*. 28 (2002) 50-58.
- [7] G.V. Belov, V.S. Iorish, V.S. Yungman, *IVTANTHERMO for Windows - database on thermodynamic properties and related software*, *CALPHAD* 23 (1999) 173-180.
- [8] P. Chaud, P.Y. Chevalier, B. Cheynet, E. Fischer, P. Mason, M. Mignanelli, *NUCLEA Database developed by THERMODATA/INPG/CNRS and AEA-T*, Contributions in Final *ENTHALPY Report*, ENTHA(03)-P018, European Commission, 5th Framework Program, Nuclear Fission (2000-2003)
- [9] Markov V.K., Verniy E.A., Vinogradov A.V. et al. *Uranium. Methods of its detection*. Edited by Prof. Markov V.K., 2nd updated edition, M., Atomizdat, 1964, 503 p., (Rus.)
- [10] *Analytical chemistry of uranium ${}_{92}\text{U}^{238}$* M. Publishing house of the USSR AS. 1962, 431 p. (Rus.)
- [11] Lukjanov V.F., Savin S.B., Nikolskaya I.V. *Photometric detection of microquantities of uranium using arsenazo III*. *ZhAKh.*, v. 15, issue 3. 1960(Rus.)
- [12] Behta S.V., Krushinov E.V., Almyashev V.I. et al. “Phase Diagram of the $\text{ZrO}_2\text{--FeO}$ System”, to be published in *Journal of Nuclear Materials*
- [13] D. Lopukh, S. Behta, A. Pechenkov et al., *New experimental results on the interaction of molten corium with core catcher material*, in: *Proc. ICONE 8 of 8th International Conference on Nuclear Engineering*, Baltimore, Maryland, USA, April 2-6, 2000, *ICONE* 8139
- [14] F.Ya. Galakhov, *High-temperature microfurnace for heterogeneous equilibria investigations in refractory oxide systems*, in: *Modern techniques of silicate and construction materials studies*. Gosstroyizdat Publishers, Moscow, 1961, pp. 178-183 (Rus.)
- [15] Behta S.V., Krushinov E.V., Almyashev V.I. et al. “ $\text{UO}_2\text{--FeO}$ phase diagram”, to be published in *Journal of Nuclear Materials*
- [16] L.P. Mezentseva, V.F. Popova, V.I. Almjashev, N.A. Lomanova, V.L. Ugolkov, S.V. Behta, V.B. Khabensky, M. Barrachin, S. Hellmann, V.V. Gusarov, “Phase diagrams of the $\text{SiO}_2\text{--Fe}_2\text{O}_3(\text{Fe}_3\text{O}_4)$ systems in different gas atmosphere”, to be published in *J. Europ. Ceram. Soc.*
- [17] Darken L.S. and Gurry R.W., *The system iron – oxygen. II. Equilibrium and thermodynamics of liquid oxide and other phases*. *J.Am.Chem.Soc.* 1946, 68, 798-816

- [18] V.B. Khabensky, S.V. Bechta, V.S. Granovsky et al., "Investigation of Corium Melt Interaction with NPP Reactor Vessel Steel (METCOR)," ISTC Project № 833-99. ISTC Final Technical Report (2001).
- [19] S.V. Bechta, V.B. Khabensky, S.A. Vitol et al., "Corrosion of Vessel Steel During its Interaction with Molten Corium.- Part 1: Experimental," to be published in Nucl. Eng. Des., reg.#BDT-025, (2005)
- [20] S.V. Bechta, V.B. Khabensky, S.A. Vitol et al., "Corrosion of Vessel Steel During its Interaction with Molten Corium.- Part 2: Model Development," to be published in Nucl. Eng. Des., reg.#BDT-026, (2005).
- [21] S.V. Bechta, V.B. Khabensky, V.S. Granovsky et al., "New Experimental Results on the Interaction of Molten Corium with Reactor Vessel Steel", Proceedings of ICAPP '04, Pittsburgh, PA USA, June 13-17, 2004, Paper 4114
- [22] B. Adroguer et al., Corium Interaction and Thermochemistry (CIT Project), In-vessel Cluster, Report INV-CIT(99)-P041 (1999)
- [23] W.A. Fischer, A. Hoffmann, Archiv fuer Eisenhuettenwesen, 28, 11, 739-743 (1957)
- [24] S. Hellmann, New Experiments on the Interaction of ZrO₂ Material with Corium Melts, Corium Interaction and Thermochemistry (CIT Project), In-vessel Cluster, Report EU-INV-CIT(99)-P037, February 2000